


 Cite this: *Chem. Commun.*, 2025, 61, 338

 Received 12th September 2024,
 Accepted 28th November 2024

DOI: 10.1039/d4cc04719b

rsc.li/chemcomm

Efficient pathways to improve electrode performance of P'2 Na_{2/3}MnO₂ for sodium batteries†

 Yosuke Ugata,[‡] Tomohiro Kuriyama^{‡,a} and Naoaki Yabuuchi^{‡,ab}

A Mn-based sodium-containing layered oxide, P'2-type Na_{2/3}MnO₂, is revisited as a positive electrode material for sodium-ion batteries, and factors affecting its electrochemical performances are examined. The cyclability of Na_{2/3}MnO₂ is remarkably improved by increasing the lower cut-off voltage during cycling even though the reversible capacity is sacrificed. Furthermore, the use of highly concentrated electrolytes, in which the presence of free solvent molecules is eliminated, effectively suppresses the dissolution of Mn ions, thus enabling stable cycling with >85% capacity retention for 300 continuous cycles.

In recent years, the rapid growth in the market of electric vehicles has resulted in an increase in the prices for lithium, cobalt, and nickel resources used in lithium-ion batteries. Therefore, great research effort has been conducted to explore new battery systems based on more abundant resources with lower costs. Recently, rechargeable sodium-ion batteries have been attracting much attention for energy storage applications in terms of abundant resources. In the past decade, numerous research efforts have been devoted to developing cost-effective and high-performance electrode materials, especially for positive electrodes, made from earth abundant elements.^{1–3} Among a variety of potential positive electrode materials, layered sodium transition metal oxides (Na_xMeO₂, Me = transition metal ions) have been intensively studied.^{4,5} From the viewpoint of material abundance and energy density, Mn-based layered oxides (Na_xMnO₂) are considered to be promising positive electrode candidates. The structure of layered Na_xMnO₂ is divided into two groups with different layered stacking manners, O3-type and

P2-type, based on Delmas's notation.⁶ Here, the letter "O" or "P" denotes the octahedral or prismatic site accommodating Na ions between MnO₂ slabs, and the number "2" or "3" represents the number of MnO₂ slabs in a cell unit. An in-plane distorted O3-type, denoted as O'3-type, NaMnO₂ delivers a relatively large reversible capacity approaching 200 mA h g⁻¹.⁷ However, the reversible capacity fades upon cycling due to the dissolution of Mn ions into electrolyte solutions and internal stress generated by structural changes on electrochemical cycles.^{8,9} On the other hand, compared with O'3-type NaMnO₂, P'2-type Na_{2/3}MnO₂ shows better cyclability without sacrificing a large reversible capacity over 200 mA h g⁻¹, but its cyclability is still unacceptable as an electrode material for practical applications.^{10,11} In this study, P'2 Na_{2/3}MnO₂ is revisited as a positive electrode material for battery applications. The cycling performance of P'2 Na_{2/3}MnO₂ is significantly improved by controlling the operating voltage during electrochemical cycling. In addition, the use of highly concentrated electrolytes enables highly reversible and stable cycling of P'2 Na_{2/3}MnO₂ for 300 continuous cycles with a large reversible capacity, ~200 mA h g⁻¹. On the basis of these results, factors affecting the electrode performance of P'2 Na_{2/3}MnO₂ and its practical feasibility are discussed.

P'2-type Na_{2/3}MnO₂ was synthesized by a solid-state reaction. Starting materials composed of Na₂CO₃ (FUJIFILM Wako Pure Chemical) and MnCO₃·*n*H₂O (FUJIFILM Wako Pure Chemical) were mixed by wet ball milling with ethanol and then dried in air. A mixture of the precursors was pressed into a pellet at 20 MPa, and the obtained pellet was heated at 1050 °C for 12 h in air followed by quenching to room temperature.¹¹ Fig. 1a shows a synchrotron X-ray diffraction pattern of the synthesized Na_{2/3}MnO₂. Synchrotron XRD measurement was conducted at the beamline BL5S2 in the Aichi Synchrotron Radiation Center (AichiSR) in Japan. The sample powder was sealed in a glass capillary in an Ar atmosphere and measured using the 2D detector (PILATUS 100 K, DECTRIS Ltd). The wavelength of X-rays was 0.775 Å. An XRD pattern of the sample is assigned into a single-phase P'2-type layered structure with a space group of *Cmcm*. Note that the ratio of *b/a* values is higher than √3,

^a Department of Chemistry and Life Science, Yokohama National University, 79-5 Tokiwadai, Hodogaya-ku, Yokohama 240-8501, Japan.

E-mail: yabuuchi-naoaki-pw@ynu.ac.jp

^b Advanced Chemical Energy Research Center (ACERC), Institute of Advanced Sciences, Yokohama National University, 79-5 Tokiwadai, Hodogaya-ku, Yokohama 240-8501, Japan

† Electronic supplementary information (ESI) available. See DOI: <https://doi.org/10.1039/d4cc04719b>

‡ These authors contributed equally to this work.





Fig. 1 (a) A synchrotron XRD pattern of $\text{Na}_{2/3}\text{MnO}_2$ and (b) schematic illustration of the P'2-type layered structure, which was drawn using the program, VESTA.¹² (c) A SEM image and (d) HAADF- and (e) ABF-STEM images of magnified regions of Fig. S1 (ESI[†]) along [100] for $\text{Na}_{2/3}\text{MnO}_2$.

indicating an in-plane structural distortion induced by Jahn-Teller active Mn^{3+} ions (Fig. 1b).¹¹ From a morphological observation using a scanning electron microscope (JCM-6000, JEOL), P'2 $\text{Na}_{2/3}\text{MnO}_2$ consists of mainly large particles with a size of $> 10 \mu\text{m}$ and partially small particles ($< 5 \mu\text{m}$) in Fig. 1c. The crystal structure of P'2 $\text{Na}_{2/3}\text{MnO}_2$ was further characterized by high-angle annular dark field (HAADF) and annular bright field (ABF) scanning transmission electron microscopy (STEM) using a JEOL JEM-ARM200F instrument equipped with a spherical aberration corrector operated at an acceleration voltage of 200 kV (Fig. 1d, e and Fig. S1, ESI[†]). In a HAADF-STEM image viewed along [100], heavier Mn ions are clearly highlighted as bright spots (Fig. 1d), and their arrangement along the *c*-axis direction is in good agreement with the P2-type layered stacking sequence. In contrast, for an ABF-STEM image, lighter O and Na ions are also distinctly visualized as dark spots (Fig. 1e).

The electrochemical performance of P'2 $\text{Na}_{2/3}\text{MnO}_2$ was examined in two-electrode electrochemical cells with metallic sodium. The configuration of the two-electrode cell is described in the ESI[†]. Galvanostatic charge/discharge tests of Na/ $\text{Na}_{2/3}\text{MnO}_2$ cells were performed with two different lower cut-off voltages, 1.5 and 2.4 V, and a fixed upper cut-off voltage of 4.0 V at a current rate of 10 mA g^{-1} . The corresponding charge/discharge curves are shown in Fig. 2a. In the first cycle, the cell discharged to 1.5 V shows a reversible capacity of over 200 mA h g^{-1} , which is consistent with that of a previous report.¹¹ However, in the subsequent cycles, a gradual increase in polarization on the charge/discharge process is observed upon cycling, and 35% of the initial reversible capacity is lost after 30 cycles (Fig. 2b). In contrast, when the lower cut-off voltage is increased to 2.4 V, the increased polarization and capacity fading with cycling are significantly mitigated even though the reversible capacity is limited to approximately 60% of that in the cell with a 1.5 V cut-off. Moreover, coulombic efficiency is also improved, ~ 98 and 93% on average for 2.4 and 1.5 V cut-off, respectively, as shown in Fig. 2c. In differential capacity plots shown in Fig. 2d, a stepwise charge/discharge

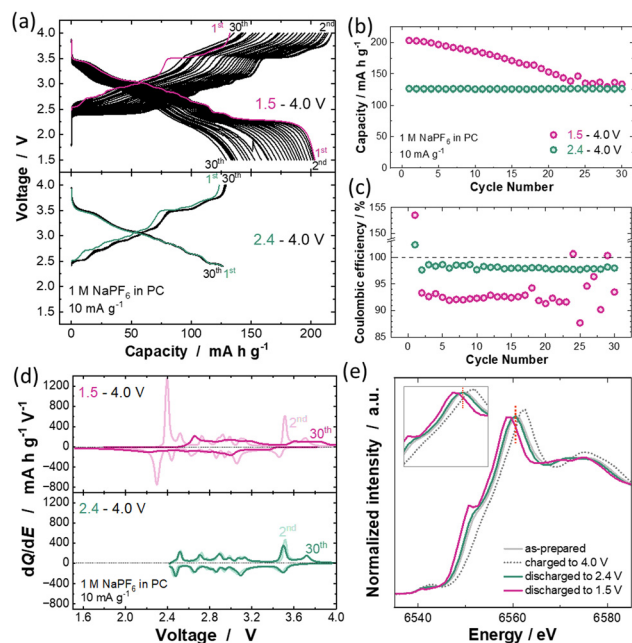


Fig. 2 (a) Charge/discharge curves, (b) capacity retention, (c) coulombic efficiency, and (d) differential capacity plots of P'2 $\text{Na}_{2/3}\text{MnO}_2$ cycled with 1 M NaPF_6 in propylene carbonate (PC) electrolyte in the voltage ranges of 1.5–4.0 V and 2.4–4.0 V at a rate of 10 mA g^{-1} . (e) Changes in Mn K-edge XAS spectra for P'2- $\text{Na}_{2/3-y}\text{MnO}_2$ on electrochemical cycles.

profile is lost after 30 cycles in the voltage range of 1.5–4.0 V, but mostly maintained in the range of 2.4–4.0 V. In general, the dissolution of Mn ions into electrolyte solution is considered as a major degradation mechanism of Mn-based electrode materials.^{13,14} Moreover, the dissolved Mn ions deposit on the negative electrode surface,¹⁵ and deposited Mn causes the electrolyte decomposition and formation of by-products, for instance, alkoxide species.¹⁶ When the by-products are soluble species into electrolytes, they are oxidatively decomposed at the surface of the positive electrode, leading to lower coulombic efficiency. Because the same upper cut-off voltage, 4.0 V, is used for both tests, the difference is found with the accumulation of Mn^{3+} ions for the sample with 1.5 V cut-off. Similarly, the electrode reversibility for a spinel-type oxide, LiMn_2O_4 , is influenced by the average oxidation states for Mn ions, and much better electrode reversibility is achieved for $\text{Li}_{1-x}\text{Mn}_{2-x}\text{O}_4$ and $\text{LiMg}_x\text{Mn}_{2-x}\text{O}_4$ with higher Mn oxidation states.¹⁷ Such high reversibility for spinel-type oxides with higher Mn valence is attributed to the smaller amount of Mn dissolution.¹⁸ According to the first-principles computational study, the higher Mn oxidation state increases the covalency and decreases the anti-bonding nature for Mn and O bonds, which energetically stabilize Mn–O bonds and reduce Mn dissolution.¹⁹ Therefore, increasing the lower cut-off voltage maintains a higher average oxidation state of Mn ions in the electrode (*i.e.*, a larger $\text{Mn}^{4+}/\text{Mn}^{3+}$ ratio), thereby mitigating the Mn dissolution into the electrolyte and resulting in superior cyclability for the sample with 2.4 V cut-off. In fact, brown coloration of the glass filter used as a separator associated with Mn dissolution is found



